HHS Public Access

Author manuscript

Clin Cancer Res. Author manuscript; available in PMC 2018 August 01.

Published in final edited form as:

Clin Cancer Res. 2017 August 01; 23(15): 4473–4481. doi:10.1158/1078-0432.CCR-16-2655.

Immune microenvironment in microsatellite instable endometrial cancers: Hereditary or sporadic origin matters

Janelle B. Pakish[1], **Qian Zhang**[1], **Zhongyuan Chen**[2], **Han Liang**[3], **Gary B. Chisholm**[1], **Ying Yuan**[4], **Samuel C. Mok**[1], **Russell R. Broaddus**[5], **Karen H. Lu**[1,+], and **Melinda S. Yates**[1,*,+]

[1]Department of Gynecologic Oncology and Reproductive Medicine, The University of Texas MD Anderson Cancer Center, Houston, TX

[2]Department of Statistics, George R. Brown School of Engineering, Rice University, Houston, TX

[3]Department of Bioinformatics and Computational Biology, The University of Texas MD Anderson Cancer Center, Houston, TX

[4]Department of Biostatistics, The University of Texas MD Anderson Cancer Center, Houston, TX

[5]Department of Pathology, The University of Texas MD Anderson Cancer Center, Houston, TX

Abstract

Purpose—Recent studies show that colorectal tumors with high microsatellite instability (MSI-H) have increased immunogenicity and response to immunotherapy compared to microsatellite stable (MSS) tumors. It is not yet clear if MSI-H endometrial cancer (EC) may also benefit from these therapies. It is also unknown whether immune response is equivalent in MSI-H EC with sporadic or inherited Lynch syndrome origins.

Experimental Design—Multiplexed fluorescent immunohistochemistry (IHC) was used to compare matched MSI-H (n=60) and MSS (n=96) EC specimens by evaluating immune cell populations in tumor and stroma compartments. Sporadic MSI-H and Lynch syndrome-associated (LS) MSI-H EC were also directly compared.

Results—Increased immune cells were present in stroma of MSI-H EC compared to MSS, including granzyme B^+ cells, activated cytotoxic T lymphocytes (CTLs, $CD8^+$granzyme B^+), and PD-$L1^+$ cells. Granzyme B^+ cells and activated CTLs were also increased in the tumor compartment of MSI-H ECs. Comparing sporadic and LS MSI-H EC showed distinct differences in immune cell populations, indicating that mechanisms underlying microsatellite instability alter immune response. Specifically, LS MSI-H EC showed increased $CD8^+$ cells and activated CTLs in stroma, with reduced macrophages in stroma and tumor compared to sporadic MSI-H. Sporadic MSI-H had increased PD-$L1^+$ macrophages in stroma and tumor compared to LS MSI-H EC.

Conclusions—MSI-H EC has increased immune cell infiltration compared to MSS EC and the hereditary or sporadic origin of microsatellite instability impacts immune response. Clinical trials

*Corresponding Author: Melinda S. Yates, PhD, Department of Gynecologic Oncology and Reproductive Medicine, 1155 Hermann Pressler Dr., Unit 1362, Houston, TX 77030, Phone: 713-745-0123, Fax: 713-792-7586, msyates@mdanderson.org.
+These authors contributed equally to the manuscript.

to determine the role of immunotherapy in patients with MSI-H EC must evaluate Lynch-related and sporadic MSI-H tumors separately.

Keywords

Uterine cancer; microsatellite instability; immune microenvironment; hereditary cancers; Lynch syndrome

Introduction

Anti-tumor immune response is thought to be associated with high somatic mutational load, which causes increased production of tumor-specific neoantigens (1). In fact, tumors with high mutation rates, such as melanoma, have proven responsive to immunotherapy. Immunotherapy strategies against tumors with high microsatellite instability (MSI-H) are currently being studied due to the high mutational load inherent to this tumor subtype as well. MSI-H tumors have defects in DNA mismatch repair (MMR), which result in errors in areas of repetitive DNA sequences, known as microsatellites (2). Howitt et al. described prediction models that indicate MSI-H EC has a 7-fold higher neoantigen load compared to microsatellite stable (MSS) tumors (3). MMR deficiency may occur sporadically due to *MLH1* promoter methylation or from germline mutations in MMR genes (*MLH1*, *MSH2*, *MSH6*, *PMS2*, *EPCAM*) seen in Lynch syndrome. MSI-H status is seen most frequently in colorectal and endometrial cancers.

Although MSI-H tumors occur in colorectal and endometrial cancers due to either sporadic *MLH1* promoter methylation or inherited Lynch syndrome, previous studies have not evaluated potential differences in anti-tumor response based on the origin of these tumors. Recent studies of the immune microenvironment in an overall cohort of MSI-H EC and ultramutated EC (related to *DNA Polymerase ε* mutation) have shown increased tumor infiltration lymphocytes (TILs) compared to MSS ECs (3,4). Colorectal cancer studies have also shown that MSI-H tumors have increased density of TILs and cytotoxic T lymphocytes (CTLs) compared to MSS tumors, but again did not evaluate *MLH1* methylated and Lynch syndrome cases separately (5,6). Additionally, elevated immune checkpoint expression of PD-1 and PD-L1 has been demonstrated in the immune microenvironment of MSI-H colorectal tumors (5) and led to an anti-PD-1 clinical trial. A phase II study of PD-1 blockade using pembrolizumab in colorectal cancers showed improved immune-related objective response rates among MSI-H compared to MSS tumors (7).

Previous studies have focused on the role of increased production of neoantigens due to increased mutational load as a driver for anti-tumor activation. As such, sporadic *MLH1* methylated and Lynch syndrome-associated MSI-H tumors were not analyzed separately; however, this assumption has not been tested. In fact, it is well recognized that MSI-H colorectal cancers do not represent a single molecularly homogeneous subgroup. Approximately 70–80% of MSI-H colorectal cancers can be categorized into a unique subgroup of cases with widespread hypermethylation, called the CpG island methylator phenotype (CIMP) (8). These cases show hypermethylation of CpG islands in the promoter of tumor suppressor genes and inactivation of *MLH1* due to aberrant promoter methylation,

but CIMP colorectal cancers have different histology, a distinct molecular profile associated with *BRAF* mutation, and unique clinical characteristics despite some overlapping features with the MSI-H subtype (9–11). The methylator phenotype has not yet been well described in endometrial cancer (12,13). Again looking to the colorectal cancer literature, the observation that there are distinct molecular subgroups of MSI-H tumors (14,15) suggests that this assumption of an identical immune response across all MSI-H tumors may be doubtful. The study reported here sought to use robust methodologies to characterize the immune microenvironment of sporadic *MLH1* methylated and Lynch syndrome-associated MSI-H EC as a means to begin to determine whether microsatellite instability drives equivalent immune activation, regardless of sporadic or hereditary origin. Differences in immune microenvironment between sporadic and Lynch syndrome-associated MSI-H EC and MSS EC will provide opportunities to identify candidate subgroups for targeted immunotherapeutic regimens.

Over 10,000 women will die from endometrial cancer (EC) in the United States this year (16), largely because of resistance to therapy in the advanced/recurrent disease setting. Combination chemotherapy in these circumstances offers response rates (RR) ranging from 30–60% and median progression free survival of 5–14 months (17). In patients that progress despite chemotherapy, available therapies are extremely limited and RR of only 9–32% are achieved with second line therapies (17–20). For this reason, it is critical to identify molecular subgroups that are amenable to targeted therapies, including immunotherapy.

Materials and Methods

Patients and Tumor Specimens

This study was conducted with approval from the institutional review board of The University of Texas MD Anderson Cancer Center. MSI-H endometrial cancer specimens from 2000–2015 were identified from archived samples in the Gynecologic Oncology tumor bank and Lynch syndrome patient registry. MSI tumor status was determined clinically using a method developed by the Molecular Diagnostic Laboratory at MD Anderson Cancer Center that has been previously described (21) and results were reported in the medical record. Briefly, MSI testing was performed following extraction of DNA from FFPE tumor and normal tissue. A polymerase chain reaction (PCR) based method was used for analysis followed by capillary electrophoretic detection of microsatellite markers. Seven microsatellite markers were used in this method. These markers included BAT25, BAT26, BAT40, D2S123, D5S346, D17S250, and TGFBR2. The number of tumor microsatellite repeats for each of the markers was compared to normal tissue from the same case. A tumor was considered MSI-H if three or more of the seven markers demonstrated allelic shift. When all markers were negative for allelic shift, the case was defined as MSS. Expression of MMR proteins (MLH1, MSH2, MSH6, PMS2) was further evaluated in tumors with microsatellite instability using standard clinical pathology procedures. Lack of protein expression of MSH2, MSH6, or PMS2 in the tumor was considered probable Lynch syndrome. For those with MLH1 loss by IHC, MLH1 promoter methylation was analyzed. Those cases showing MLH1 loss by IHC and without MLH1 promoter methylation were classified as probable Lynch syndrome. MSI-H cases were matched approximately 1:2 to

MSS EC specimens from the tumor bank. Matching was done based on histology, tumor grade, tumor stage, age at diagnosis, and body mass index (BMI). Archived formalin fixed paraffin-embedded (FFPE) tissue blocks were cut in 4 μm sections. Clinical data was abstracted from the medical record as available.

Polymerase E (POLE) sequencing

Due to previous reports indicating that *POLE* mutations in EC result in an enhanced immune response, MSS cases were further screened for *POLE* mutations. Cases with *POLE* mutation were excluded from the analysis. MSS cases that could not be fully sequenced for *POLE* (resulting in unknown *POLE* mutation status) were also excluded from analysis. *POLE* exonuclease domain mutations were assessed in FFPE tissue using polymerase chain reaction–based Sanger sequencing at The University of Texas MD Anderson Cancer Center Sequencing and Microarray Core Facility. DNA was extracted using Pico Pure DNA Extraction kit (Applied Biosystems, Foster City, CA). Primers and method were used as previously described by Billingsley et al (22).

Immunohistochemistry

Fluorescent IHC multiplexing was performed using the Opal™ multiplex system (PerkinElmer, Waltham, MA), and the protocol was adapted from that previously described (23). Briefly, antigen retrieval was carried out in a decloaking chamber for 15 minutes with specific antibody conditions as listed separately in Supplementary Table S1. Sequential incubation with each primary antibody for multiplexing was conducted at 4°C in a humidified chamber for 16 hours. After each incubation, slides were washed and species specific secondary horseradish peroxidase (HRP) (Invitrogen, Carlsbad, CA) was applied for 10 min. Slides were again washed and incubated with fluorescent tyramide signal amplification (TSA) reagent for 10 min. This was followed by washing and repeat heating in a decloaking chamber for 15 min. The next primary antibody was then applied after blocking. The process continued as previously described until all primary antibodies and corresponding TSA reagents had been applied to the slides. The slides were heated one last time in a decloaking chamber at 96°C for 15 min. After cooling and washing, DAPI was applied for 5 min and slides were cover slipped with an aqueous mounting solution (Thermo Scientific, Waltham, MA).

Three different multiplexing panels were performed with the order, primary antibody and corresponding fluorophore listed. Panel 1: (1) Granzyme B (1:300, clone 11F1, Leica, UK)/ Cyanine 3, (2) CD8 (1:400, clone 4B11, Leica)/FITC, (3) CD68 (1:500, clone KP1, Biogenex, Fremont, CA)/Cy5.5, and (4) PD-L1 (1:1600, clone E1L3N, Cell Signaling, MA)/ Cy3.5, (5) DAPI.

Panel 2: (1) CD3 (1:900, clone SP7, Thermo Scientific)/520 nm, (2) CD4 (1:450, clone 4B12, Thermo Scientific)/540 nm, (3) PD-L1/620 nm, (4) CDllc (1:1000, clone 5D11, Leica)/690 nm, and (5) DAPI.

Panel 3: (1) CD103 (1:5000, clone EPR4166, Abcam, Cambridge, MA)/520 nm, (2) CD8/620 nm, and (3) DAPI.

Due to batch differences associated with different staining conditions for the 3 multiplexing panels, comparisons between groups were only performed within an individual panel batch.

Immune cell markers were as follows: CD3 (general T cell marker), CD4 ($CD4^+$ T cells), CD8 (cytotoxic T lymphocytes, CTLs), granzyme B (activated CTLs or Natural Killer, NK, cells), CD68 (macrophages), PD-L1 (immune checkpoint ligand), CD11c (dendritic cell marker), and CD103 (intraepithelial T cell or dendritic cell marker). Co-staining was evaluated for granzyme B/CD8 (activated CTLs), CD3/CD4 (helper T cells), PD-L1/CD68 ($PD\text{-}L1^+$ macrophages), PD-L1/CD11c ($PD\text{-}L1^+$ dendritic cells), and CD8/CD103 (intraepithelial T cells).

Imaging and Analysis

Multispectral imaging was performed with the Vectra® 2 automated system (PerkinElmer) with the assistance of the Flow Cytometry and Cellular Imaging Facility at MD Anderson. With this system, an algorithm was created to capture up to 30 random high powered fields of tumor-containing images. Four filters were used to capture images (DAPI, Cy3, FITC, and Cy5), and optimal exposure times were determined for each filter individually.

Following image acquisition, inForm® software version, 2.1.5430.24864 (PerkinElmer) was used to create a spectral library from each of the single fluorophore slides to allow for unmixing of the fluorophore images. A sample set of images was used to define areas of tumor epithelium and stroma, and train the inForm® software in tissue segment pattern recognition. DAPI staining was used to identify nuclei within each of the tissue compartments, and as a reference to determine cellular cytoplasm and membrane segmentation based on the inForm® algorithm. Thresholds and scoring were defined by fluorescent pixel intensity that accurately identified positive staining cells, as determined by manual review of sample images for each of the antibodies. Positive cell staining was also determined based on the target cellular compartment for each of the specific antibodies. Thresholds for each of the antibodies are as follows and values greater than the listed threshold were considered positive staining. Panel 1: granzyme B/Cy3 (membrane score >3), CD8/FITC (membrane score >2), CD68/Cy5.5 (cytoplasm score >1), PD-L1/Cy3.5 (cytoplasm score >5). Panel 2: CD3/520 nm (membrane score >0.83), CD4/540 nm (membrane score >0.33), PD-L1/620 nm (cytoplasm score >2.5), and CD11c/690 nm (membrane score >0.2). Panel 3: CD103/520 nm (membrane score >2.0) and CD8/620 nm (membrane score >4.5).

An algorithm to determine positive cell counts within the stroma and tumor epithelial compartment was created using the discussed tissue and cell segmentation and fluorescent pixel intensity algorithm using the inForm® software. This algorithm was applied to all images. A reviewer blinded to MSI status manually reviewed all images to assess accuracy of the algorithm. Those images that were determined to be inaccurate were added back to the training set to improve segmentation accuracy. Due to the inherent variation of tissue architecture among samples, 100% segmentation accuracy was unable to be obtained and those images with gross segmentation inaccuracy were excluded from the algorithm. Overall there was an average of 16 images analyzed per specimen (range 1–35). Additionally, tissue

degradation secondary to multiple rounds of heating occurred in some cases and these cases were removed from the analysis.

The number of positive staining cells for each of the antibodies was then calculated per millimeter squared (mm^2) within both the tumor epithelium and the tumor-associated stroma for each of the cases using code written in SAS version 9.4 (Cary, NC).

Statistical Analysis

Statistical analysis was performed using GraphPad Prism version 6 (GraphPad Software, La Jolla, California) and Stata version 14.1 (StataCorp, College Station, TX). The Mann-Whitney and chi-squared tests were used to compare demographic data between the two groups as indicated. For comparison of immune cell markers between MSI-H and matched MSS cases, the Wilcoxon matched-pairs signed rank test was used. Values for each MSI-H case were paired with the matched MSS case. In the case that more than one matched MSS case was available, the average of the matches was used for comparison. The overall number of cases is indicated at the top of each data table; however, when a case was excluded for any reason, the corresponding matched MSS or MSI-H case was also removed from the analysis for that marker. Lynch syndrome MSI-H and sporadic MSI-H cases were compared as a group (not matched) and the Mann-Whitney test was used for this comparison. A p value of <0.05 was used to signify statistical significance. Box plots were created to visualize data for percent positive PD-L1 staining cells. The upper border of the box represents the third quartile, the lower border the first quartile, and the line the median. The whiskers are defined using the Tukey box plot method where whiskers represent 1.5 times the upper and lower interquartile range. Study data were collected and managed using REDCap electronic data capture tools (24) hosted at The University of Texas MD Anderson Cancer. REDCap (Research Electronic Data Capture) is a secure, web-based application designed to support data capture for research studies.

Results

Specimens and demographics

Evaluation of EC immune microenvironment was conducted using specimens from the gynecologic oncology archived tumor bank and Lynch syndrome patient registry. In total, 60 MSI-H cases were identified and matched approximately 1:2 to 107 MSS cases. Further testing of MSS cases was performed to exclude *POLE* mutant cases (n=4) or cases with unknown *POLE* status (n=7), resulting in 96 matched MSS cases. Of the MSI-H cases, 20 were found to have IHC defects in MMR genes consistent with probable Lynch syndrome (LS) and this group was used for the LS MSI-H sub-analysis. A summary of Lynch syndrome testing characteristics for these cases is shown in Supplementary Table S2. One MSI-H case had loss of MSH2 and MSH6 on IHC, but no germline deleterious mutations of DNA MMR genes. Another MSI-H case had unknown specific protein loss, but was positive for microsatellite instability with allelic shift in 5 of 7 microsatellite markers. These last two cases were included only in the overall MSI-H versus MSS analysis. 38 MSI-H cases demonstrated sporadic promoter methylation of MLH1 and were used for the sporadic MSI-H sub-analysis.

There were no significant differences in characteristics used for case matching of MSI-H to MSS (histology, age at diagnosis, BMI, stage, and grade) as shown in Table 1. Some clinical data could not be obtained for a portion of the MSI-H cases, primarily the LS cases. Many LS MSI-H EC cases were obtained from a Lynch syndrome patient registry, which included specimens collected from outside institutions and had more limited clinical information available. As shown in Table 1, 11 cases were missing details of depth of myometrial invasion and 12 were missing LVSI information. As comparison of depth of invasion and LVSI were not primary objectives, these cases were not excluded from the cohort. In addition, BMI data was missing for 13 LS cases, 2 cases had unknown grade (both LS MSI-H) and 5 had unknown stage (all LS MSI-H). However, these cases were matched according to the data available and were included in the analysis given the limited number of cases of the LS MSI-H subtype.

Overall, the majority of cases were stage IA in both groups (MSI-H 58.3% vs MSS 68.8%; p=0.76) and the majority of cases were grade 2 (MSI-H 68.3% vs MSS 76.0%; p=0.42). As most cases were stage IA, only 25.0% had myometrial invasion equal to or greater than 50% in the MSI-H and 27.1% in the MSS cases. Lastly, there was a significant difference in lymphovascular space invasion (LVSI) between the two groups with more MSS cases being absent LVSI (69.8%) than that seen in the MSI-H (38.3%) cases (p=0.01).

Comparison of overall cohort of MSI-H endometrial cancers versus matched MSS

Differences in immune cell markers between all MSI-H and MSS EC was examined using three fluorescent IHC multiplexing panels. A representative image for each multiplexing panel is demonstrated in Supplementary Figure S1. The number of positive staining cells for each of the markers in both the stromal and tumor epithelial compartments in all MSI-H versus MSS EC is shown in Table 2. Among all MSI-H tumors, the median number of granzyme B^+, PD-$L1^+$, $CD3^+$, and $CD4^+$ staining cells were significantly higher within the tumor-associated stroma compared to MSS EC. Tumor epithelial $CD8^+$ and granzyme B^+ staining was also significantly higher in all MSI-H compared to MSS EC, while $CD68^+$ staining was significantly lower in the tumor epithelial compartment of MSI-H cases. The percentage of PD-$L1^+$ cells within the two compartments was also assessed, as this value has been used as an indicator for response to immune checkpoint blocking therapies in some clinical trials. In this study, the median percentage of PD-$L1^+$ staining stromal cells was significantly increased in the MSI-H cases compared to MSS cases (60.5% vs 48.3%; p<0.01). However, in the tumor epithelium, there was no significant difference in median percentage of PD-L1 expression between the two groups (MSI-H 2.0% vs MSS 1.5%; p=0.46) (Figure 1A). No other statistically significant difference in individual staining was seen within the stromal or tumor epithelial compartment for the two groups.

Co-staining of markers was assessed within the groups and among each of the tissue compartments as shown in Table 2. Co-staining of $CD8^+$ and granzyme B^+ cells represents the number of activated CTLs, and was significantly higher in MSI-H compared to MSS cases in both the stromal and tumor epithelial compartments. Helper T cells were evaluated via co-staining of CD3/CD4. Stromal $CD3^+CD4^+$ cells were increased in MSI-H compared to MSS but showed no statistically significant differences within the tumor. Co-staining for

PD-L1$^+$ macrophages (PD-L1$^+$ and CD68$^+$) was also evaluated, and showed no significant differences. Additional staining was performed to evaluate PD-L1$^+$ dendritic cells (PD-L1$^+$ and CD11c$^+$) and CD103/CD8 (intraepithelial CD8$^+$ cells). To streamline data presentation, results for co-staining of PD-L1$^+$ dendritic cells and CD8$^+$CD103$^+$ immune cell populations, as well as separate CD11c and CD103 staining are not shown. There were no statistically significant differences for these markers in any of the group comparisons (Tables 2–5).

Comparison of sporadic MSI-H endometrial cancer with matched MSS cases

To evaluate differences in immune markers of sporadic MSI-H compared to matched MSS cases, a secondary sub-analysis was then performed excluding LS MSI-H cases. This analysis included only MSI-H EC with MLH1 promoter methylation compared to matched MSS EC. Within this subgroup, the number of granzyme B$^+$, CD3$^+$, and CD4$^+$ cells within tumor-associated stroma was higher among the sporadic MSI-H versus MSS cases (Table 3). PD-L1$^+$ cells were increased within the stroma and tumor of sporadic MSI-H versus MSS cases. The median percentage of PD-L1$^+$ staining cells (62.5% vs 46.0%; $p<0.0001$) was also significantly higher in the stromal compartment for sporadic MSI-H versus MSS cases, similar to that seen in all MSI-H cases (Figure 1B). The percentage of PD-L1$^+$ cells within the tumor epithelial compartment was also significantly different in sporadic MSI-H compared to MSS cases (2.5% vs 1.0%; $p=0.009$) (Figure 1B).

As in the evaluation of all MSI-H cases, co-staining was evaluated and a comparison of the median number of positive cells is shown in Table 3. Sporadic MSI-H cases demonstrated an increase in the median number of PD-L1$^+$ macrophages (co-staining of PD-L1 and CD68) in both stroma and tumor compared to MSS. Interestingly, this difference was not present in the overall MSI-H cohort analysis. T helper cells (co-staining of CD3 and CD4) was increased in the stroma compared to matched MSS cases.

Lynch syndrome-associated MSI-H endometrial cancer versus matched MSS

A sub-analysis of immune markers in LS MSI-H compared to matched MSS EC was conducted (Table 4). LS MSI-H EC demonstrated a significantly higher median number of CD8$^+$ staining cells in both the stromal and tumor epithelial compartments when compared to MSS EC. The number of PD-L1$^+$ cells in the tumor was significantly lower in LS MSI-H cases versus MSS cases. The median number of CD68$^+$ staining cells was found to be significantly reduced in the tumor epithelial compartment in LS MSI-H cases compared to MSS tumors. In regards to the median percentage of PD-L1$^+$ cells, there was no difference between LS MSI-H and MSS cases in the stroma (LS MSI-H 52.0% vs MSS 64.0%; $p=0.62$); however, LS cases showed a significant decrease in the percentage of PD-L1$^+$ cells in the tumor epithelial compartment (LS MSI-H 1.0% vs MSS 3.5%; $p=0.03$) (Figure 1C).

Co-staining comparison of immune markers for LS MSI-H versus MSS EC is also shown in Table 4. There was a significantly higher median number of activated CTLs (co-staining with CD8 and granzyme B) in the stroma and tumor of LS MSI-H versus MSS cases. The median number of PD-L1$^+$ macrophages was decreased in LS cases compared to MSS, in contrast to the observation in the sporadic cohort. No other significant differences were noted from co-staining analysis.

Given the intriguing differences shown between each subgroup of MSI-H EC relative to MSS EC, we then directly compared LS MSI-H and sporadic MSI-H cases to determine if the origin of microsatellite instability influences the immune microenvironment. As shown in Table 5, LS MSI-H EC had increased CD8+ cells in the stroma and reduced numbers of CD68+ macrophages in the stromal and tumor compartments compared to sporadic MSI-H EC. Co-staining revealed increased activated cytotoxic T lymphocytes in the stroma of LS MSI-H EC. Furthermore, PD-L1+ macrophages were increased in the stroma and tumor of sporadic MSI-H EC compared to LS cases. There were no significant differences in median percentage of PD-L1$^+$ cells when comparing sporadic MSI-H to LS MSI-H cases in either the stroma (sporadic MSI-H 62.5% vs 55.0% LS MSI-H; p=0.19) or tumor epithelial (sporadic MSI-H 2.0% vs 1.0% LS MSI-H; p=0.20) compartments (Figure 1D). This comparison was unmatched and differences between the two groups did exist based on the known etiology of the disease; Lynch syndrome MSI-H patients were younger than sporadic MSI-H patients (51.9 years vs 64.2 years; p<0.001) and had a different distribution of histology and grade (see Supplementary Table S3), consistent with previous reports on sporadic versus LS EC. BMI was unknown for 13 of 20 LS cases, making it difficult to reliably compare BMI in this cohort.

Discussion

A detailed and robust multiplexed fluorescent IHC examination of immune cell populations in MSI-H and MSS EC specimens was initially undertaken to identify specific differences in the immune microenvironment, and this analysis showed that anti-tumor immune response is elevated in MSI-H EC. By separately evaluating both sporadic and LS MSI-H EC cases, we were able to identify the distinct differences relative to MSS EC. This prompted further analysis of a direct comparison between the two MSI-H subtypes, which identified differences in specific T cell and macrophage populations. While the different clinicopathological characteristics of LS EC precluded a matched analysis to sporadic MSI-H EC, the altered immune cell infiltrates identified in the analysis for both subgroups compared to matched MSS EC provide further support to this observation that origin of microsatellite instability influences immune microenvironment.

In the overall analysis including all MSI-H cases, MSI-H ECs had increased granzyme B$^+$ cells and CTL activation within both the tumor epithelium and tumor-associated stroma, suggesting increased immune-mediated anti-tumor response in MSI-H ECs. Increased CD8$^+$ T cells and decreased macrophages were observed for the overall MSI-H EC cohort in the tumoral compartment. Stromal PD-L1 expression was also significantly increased in MSI-H EC and reflects immune response exhaustion and suppression.

Sub-analysis of sporadic MSI-H EC also demonstrated a difference in the immune microenvironment compared to MSS EC. Sporadic MSI-H EC had increased granzyme B$^+$ in the stroma, with increased PD-L1$^+$ cells in both tumor and stroma compared to MSS EC, reflecting increased anti-tumor response in sporadic MSI-H EC. Co-staining further revealed increased stromal helper T cells, as well as increased stromal and tumoral PD-L1$^+$ macrophages in sporadic MSI-H EC compared to MSS EC.

Comparison of the LS MSI-H subgroup versus matched MSS cases also showed increased immune activation in LS cases. This was demonstrated by increased $CD8^+$ cells and activated CTLs in the tumor and stroma of LS MSI-H versus MSS EC. The number of macrophages was decreased in the tumor epithelial compartment in LS MSI-H versus MSS EC. In contrast to the overall analysis of MSI-H cases and the sporadic MSI-H versus MSS analyses, LS MSI-H cases demonstrated no difference in PD-$L1^+$ staining in the stroma compared to MSS EC and a significant reduction in PD-$L1^+$ staining in the tumor epithelial compartment.

Our study is particularly novel in that we were able to directly compare LS MSI-H and sporadic MSI-H EC cases to evaluate distinct changes in the immune microenvironment that could be shaped by either the hereditary MMR defect or sporadic *MLH1* hypermethylation origin of microsatellite instability. This comparison revealed increased CD8+ cells and activated cytotoxic T lymphocytes in the stroma of LS compared to sporadic MSI-H cases. The number of CD68+ macrophages were decreased in the stroma and tumor of LS cases. PD-L1+ macrophages were increased in sporadic MSI-H EC in both the stroma and tumor. While a matched analysis was not possible due to the unique features of these two subgroups of EC, it is important to note that these characteristics are representative of sporadic and hereditary MSI-H EC cases overall. A limitation to this study is the number of statistical comparisons for each analysis. We report unadjusted p-values for this hypothesis-generating study, and must acknowledge the possibility of false positives and false negatives in this analysis. Importantly, the results are overall consistent with the different alterations identified when each MSI-H subgroup was compared to the matched MSS cases. While it is not yet clear how these differences could impact response to immunotherapies, these results indicate that it will be essential to evaluate response separately in both sporadic MSI-H and LS MSI-H EC. Additional studies are necessary to confirm this observation in an independent series and further probe the mechanisms underlying this heterogeneity in the MSI-H immune microenvironment.

The findings from our study provide a comprehensive view of the immune microenvironment of MSI-H EC. Previous studies of MSI-H and POLE ECs have found elevated levels of $CD3^+$ and $CD8^+$ infiltrating lymphocytes which suggests that these tumors elicit a strong immune response (3). The overall MSI-H EC analysis in our study revealed increased $CD8^+$ cells in the tumor epithelial compartment and increased $CD3^+$ cells in the stroma, there was also a significant difference in granzyme B^+ cells and activated CTLs in all MSI-H. This provides further evidence of a more active immune microenvironment in MSI-H EC, and suggests that the CTLs that are present are activated and capable of mounting an anti-tumor immune response.

Tumor-mediated immune evasion in patients with MSI-H EC was seen in our study, as evidenced by elevated PD-L1 expression among stromal cells in the overall cohort of MSI-H ECs and in the tumor and stroma of sporadic MSI-H ECs compared to matched MSS cases. Additionally, our study found low overall expression of tumor PD-$L1^+$ cells. PD-L1 expression on tumor versus stromal cells may have important implications for therapeutic response to anti-PD-L1 therapies, but expression varies among tumor types (25,26). Although many studies have focused on tumor PD-L1 expression and its ability to predict

response to anti-PD-1 and anti-PD-L1 therapy, its role as a biomarker remains unclear (25,26). In some studies, tumor PD-L1 expression has been associated with response to anti-PD-1 therapy (26). In other studies however, expression of PD-L1 on infiltrating immune cells is associated with response to anti-PD-L1 therapy rather than tumor cells (25). In our study, the increased PD-L1 expression highlights the variability of PD-L1 in the tumor microenvironment and suggests that patients with MSI-H EC may respond favorably to immune checkpoint blocking agents. Additionally, we found PD-L1$^+$ macrophages to be significantly increased in sporadic MSI-H compared to both MSS EC and LS MSI-H EC. The exact role of this subpopulation of cells in the tumor microenvironment cannot be established from our study; however, we speculate that these cells play a role in suppression of the immune response in these tumors. Additional studies are needed to characterize the role of PD-L1$^+$ immune cells in MSI-H ECs.

A previous study showed that tumors from patients with MSI-H colorectal cancer demonstrate significant immune cell expression of PD-L1 and very little tumor PD-L1 expression (5), similar to the results reported here. These findings in colon cancer have led to clinical trials of anti-PD-1 therapy in colorectal cancer that showed improved immune-related objective response rates in patients with MSI-H tumors compared to MSS tumors (7). An additional arm of this study also included patients with any MSI-H tumors, two of which were sporadic endometrial cancer patients. Both of these patients showed a response to anti-PD-1 therapy with one complete response and one partial response. Although this observation is limited to only two patients, the presence of increased stromal PD-L1 expression seen in our study further supports the use of immune checkpoint blocking agents in this population.

Unlike prior studies investigating the immune microenvironment of MSI-H tumors, our study included a unique subgroup of Lynch syndrome cases. The observation of an altered MSI-H immune microenvironment held true for analysis of both subgroups, sporadic (MLH1 methylated) and Lynch syndrome-associated MSI-H EC, but with different specific immune cell population changes in each group. In the Lynch syndrome MSI-H sub-analysis, CD8$^+$ cells and activated CTLs were increased. Yet there was a significant decrease in tumoral PD-L1 expression and no difference in stromal PD-L1 expression, in contrast to what was observed in the overall analysis and sporadic MSS ECs. This suggests that LS MSI-H ECs may have lesser response to single agent immune checkpoint blocking agents. Instead, combination of an anti-PD-1 or anti-PD-L1 agent with other immune checkpoint blocking agents may be necessary. These could include combination with anti-CTLA-4 or newer agents that are under development such as anti-TIM-3. While there are important clinical implications for the observed disparity between the immune microenvironment of LS MSI-H and sporadic MSI-H EC, further study of the mechanisms underlying these differences will be key to identifying novel immunotherapeutic strategies and identifying appropriate candidates for immunotherapy.

This study is the first to specifically address the immune microenvironment of Lynch syndrome-related EC and the largest cohort to date characterizing the immune microenvironment of MSI-H compared to MSS EC. Overall, our study demonstrates increased activity in the tumor immune microenvironment of MSI-H compared to MSS EC

tumors. In addition, this study suggests that the mechanism responsible for microsatellite instability impacts the immune microenvironment of these tumors, highlighting an important area for further study. Clinical trials investigating single and combination immune checkpoint blocking agents are needed to determine the role of immunotherapy in patients MSI-H EC and outcomes for sporadic and LS cases should be evaluated separately.

Supplementary Material

Refer to Web version on PubMed Central for supplementary material.

Acknowledgments

Sources of Support: This work was supported by the MD Anderson Uterine Cancer SPORE (P50CA098258 to KHL and RRB), a T32 training grant for gynecologic oncology (CA101642 to KHL), and by the MD Anderson Cancer Center Support Grant (CA016672) that supports the Flow Cytometry and Cellular Imaging Facility and Sequencing and Microarray Core Facility.

This work was supported by the MD Anderson Uterine Cancer SPORE (P50CA098258 to KHL and RRB), a T32 training grant for gynecologic oncology (CA101642 to KHL), and by the MD Anderson Cancer Center Support Grant (CA016672) that supports the Flow Cytometry and Cellular Imaging Facility and the Sequencing and Microarray Core Facility. The authors would like to acknowledge Dr. Jared Burks (Co-Director of the Flow Cytometry and Cellular Imaging Core Facility) for his expert assistance with multispectral imaging and quantitation systems.

References

1. Segal NH, Parsons DW, Peggs KS, Velculescu V, Kinzler KW, Vogelstein B, et al. Epitope landscape in breast and colorectal cancer. Cancer Res. 2008; 68(3):889–92. DOI: 10.1158/0008-5472.CAN-07-3095 [PubMed: 18245491]
2. Backes FJ, Leon ME, Ivanov I, Suarez A, Frankel WL, Hampel H, et al. Prospective evaluation of DNA mismatch repair protein expression in primary endometrial cancer. Gynecol Oncol. 2009; 114(3):486–90. http://dx.doi.org/10.1016/j.ygyno.2009.05.026. [PubMed: 19515405]
3. Howitt BE, Shukla SA, Sholl LM, Ritterhouse LL, Watkins JC, Rodig S, et al. Association of Polymerase e-Mutated and Microsatellite-Instable Endometrial Cancers With Neoantigen Load, Number of Tumor-Infiltrating Lymphocytes, and Expression of PD-1 and PD-L1. JAMA Oncol. 2015; doi: 10.1001/jamaoncol.2015.2151
4. van Gool IC, Eggink FA, Freeman-Mills L, Stelloo E, Marchi E, de Bruyn M, et al. POLE Proofreading Mutations Elicit an Antitumor Immune Response in Endometrial Cancer. Clin Cancer Res. 2015; 21(14):3347–55. DOI: 10.1158/1078-0432.CCR-15-0057 [PubMed: 25878334]
5. Llosa NJ, Cruise M, Tam A, Wicks EC, Hechenbleikner EM, Taube JM, et al. The Vigorous Immune Microenvironment of Microsatellite Instable Colon Cancer Is Balanced by Multiple Counter-Inhibitory Checkpoints. Cancer Discovery. 2015; 5(1):43–51. DOI: 10.1158/2159-8290.cd-14-0863 [PubMed: 25358689]
6. Phillips SM, Banerjea A, Feakins R, Li SR, Bustin SA, Dorudi S. Tumour-infiltrating lymphocytes in colorectal cancer with microsatellite instability are activated and cytotoxic. British Journal of Surgery. 2004; 91(4):469–75. DOI: 10.1002/bjs.4472 [PubMed: 15048750]
7. Le DT, Uram JN, Wang H, Bartlett BR, Kemberling H, Eyring AD, et al. PD-1 Blockade in Tumors with Mismatch-Repair Deficiency. New England Journal of Medicine. 2015; 372(26):2509–20. DOI: 10.1056/NEJMoa1500596 [PubMed: 26028255]
8. Juo YY, Johnston FM, Zhang DY, Juo HH, Wang H, Pappou EP, et al. Prognostic value of CpG island methylator phenotype among colorectal cancer patients: a systematic review and meta-analysis. Annals of oncology: official journal of the European Society for Medical Oncology/ ESMO. 2014; 25(12):2314–27. DOI: 10.1093/annonc/mdu149
9. Dahlin AM, Palmqvist R, Henriksson ML, Jacobsson M, Eklof V, Rutegard J, et al. The role of the CpG island methylator phenotype in colorectal cancer prognosis depends on microsatellite

instability screening status. Clin Cancer Res. 2010; 16(6):1845–55. DOI: 10.1158/1078-0432.CCR-09-2594 [PubMed: 20197478]

10. Jia M, Gao X, Zhang Y, Hoffmeister M, Brenner H. Different definitions of CpG island methylator phenotype and outcomes of colorectal cancer: a systematic review. Clinical epigenetics. 2016; 8:25.doi: 10.1186/s13148-016-0191-8 [PubMed: 26941852]
11. Weisenberger DJ, Siegmund KD, Campan M, Young J, Long TI, Faasse MA, et al. CpG island methylator phenotype underlies sporadic microsatellite instability and is tightly associated with BRAF mutation in colorectal cancer. Nat Genet. 2006; 38(7):787–93. DOI: 10.1038/ng1834 [PubMed: 16804544]
12. Whitcomb BP, Mutch DG, Herzog TJ, Rader JS, Gibb RK, Goodfellow PJ. Frequent HOXA11 and THBS2 promoter methylation, and a methylator phenotype in endometrial adenocarcinoma. Clin Cancer Res. 2003; 9(6):2277–87. [PubMed: 12796396]
13. Zhang QY, Yi DQ, Zhou L, Zhang DH, Zhou TM. Status and significance of CpG island methylator phenotype in endometrial cancer. Gynecologic and obstetric investigation. 2011; 72(3): 183–91. DOI: 10.1159/000324496 [PubMed: 21968189]
14. Kim JH, Rhee YY, Bae JM, Kwon HJ, Cho NY, Kim MJ, et al. Subsets of microsatellite-unstable colorectal cancers exhibit discordance between the CpG island methylator phenotype and MLH1 methylation status. Mod Pathol. 2013; 26(7):1013–22. DOI: 10.1038/modpathol.2012.241 [PubMed: 23370766]
15. Kim JH, Kang GH. Molecular and prognostic heterogeneity of microsatellite-unstable colorectal cancer. World J Gastroenterol. 2014; 20(15):4230–43. DOI: 10.3748/wjg.v20.i15.4230 [PubMed: 24764661]
16. Cancer Facts & Figures. Atlanta: American Cancer Society; 2016.
17. Bradford LS, Rauh-Hain JA, Schorge J, Birrer MJ, Dizon DS. Advances in the management of recurrent endometrial cancer. American journal of clinical oncology. 2015; 38(2):206–12. DOI: 10.1097/COC.0b013e31829a2974 [PubMed: 23764681]
18. Dellinger TH, Monk BJ. Systemic therapy for recurrent endometrial cancer: a review of North American trials. Expert Rev Anticancer Ther. 2009; 9(7):905–16. DOI: 10.1586/era.09.54 [PubMed: 19589030]
19. Dizon DS. Treatment options for advanced endometrial carcinoma. Gynecol Oncol. 2010; 117(2): 373–81. DOI: 10.1016/j.ygyno.2010.02.007 [PubMed: 20223510]
20. Slomovitz BM, Jiang Y, Yates MS, Soliman PT, Johnston T, Levenback CF, et al. A Phase II Study of Everolimus and Letrozole in Patients with Recurrent Endometrial Carcinoma. J Clin Oncol. 2015; 33(8):930–6. [PubMed: 25624430]
21. Vilar E, Mork ME, Cuddy A, Borras E, Bannon SA, Taggart MW, et al. Role of microsatellite instability-low as a diagnostic biomarker of Lynch syndrome in colorectal cancer. Cancer Genet. 2014; 207(10–12):495–502. DOI: 10.1016/j.cancergen.2014.10.002 [PubMed: 25432668]
22. Billingsley CC, Cohn DE, Mutch DG, Stephens JA, Suarez AA, Goodfellow PJ. Polymerase varepsilon (POLE) mutations in endometrial cancer: clinical outcomes and implications for Lynch syndrome testing. Cancer. 2015; 121(3):386–94. DOI: 10.1002/cncr.29046 [PubMed: 25224212]
23. Stack EC, Wang C, Roman KA, Hoyt CC. Multiplexed immunohistochemistry, imaging, and quantitation: a review, with an assessment of Tyramide signal amplification, multispectral imaging and multiplex analysis. Methods. 2014; 70(1):46–58. DOI: 10.1016/j.ymeth.2014.08.016 [PubMed: 25242720]
24. Harris PA, Taylor R, Thielke R, Payne J, Gonzalez N, Conde JG. Research electronic data capture (REDCap)--a metadata-driven methodology and workflow process for providing translational research informatics support. Journal of biomedical informatics. 2009; 42(2):377–81. DOI: 10.1016/j.jbi.2008.08.010 [PubMed: 18929686]
25. Herbst RS, Soria JC, Kowanetz M, Fine GD, Hamid O, Gordon MS, et al. Predictive correlates of response to the anti-PD-L1 antibody MPDL3280A in cancer patients. Nature. 2014; 515(7528): 563–7. DOI: 10.1038/nature14011 [PubMed: 25428504]
26. Taube JM, Klein A, Brahmer JR, Xu H, Pan X, Kim JH, et al. Association of PD-1, PD-1 ligands, and other features of the tumor immune microenvironment with response to anti-PD-1 therapy.

Clin Cancer Res. 2014; 20(19):5064–74. DOI: 10.1158/1078-0432.CCR-13-3271 [PubMed: 24714771]

Statement of translational relevance

Endometrial cancers (EC) with high microsatellite instability (MSI-H) have increased anti-tumor immune response compared to microsatellite stable (MSS) tumors. The mechanism responsible for microsatellite instability (sporadic MLH1 methylation or Lynch syndrome-associated inherited defects in DNA mismatch repair genes) impacts the immune response in these tumors. PD-L1+ cells are increased in sporadic MSI-H ECs compared to MSS, but not in Lynch syndrome cases. This suggests that patients with Lynch syndrome MSI-H EC may have lesser response to single agent anti-PD-1 or anti-PD-L1 therapies, and combination with other immune checkpoint blocking agents may be necessary. T cell populations and macrophages are also different in these two MSI-H subgroups. Ongoing immunotherapy trials must evaluate outcomes separately for sporadic and Lynch syndrome MSI-H EC, and other MSI-H tumor types (colon, gastric). Although MSI-H EC have increased anti-tumor immune response, the sporadic or Lynch syndrome subtype may dictate responsiveness to specific immunotherapy agents.

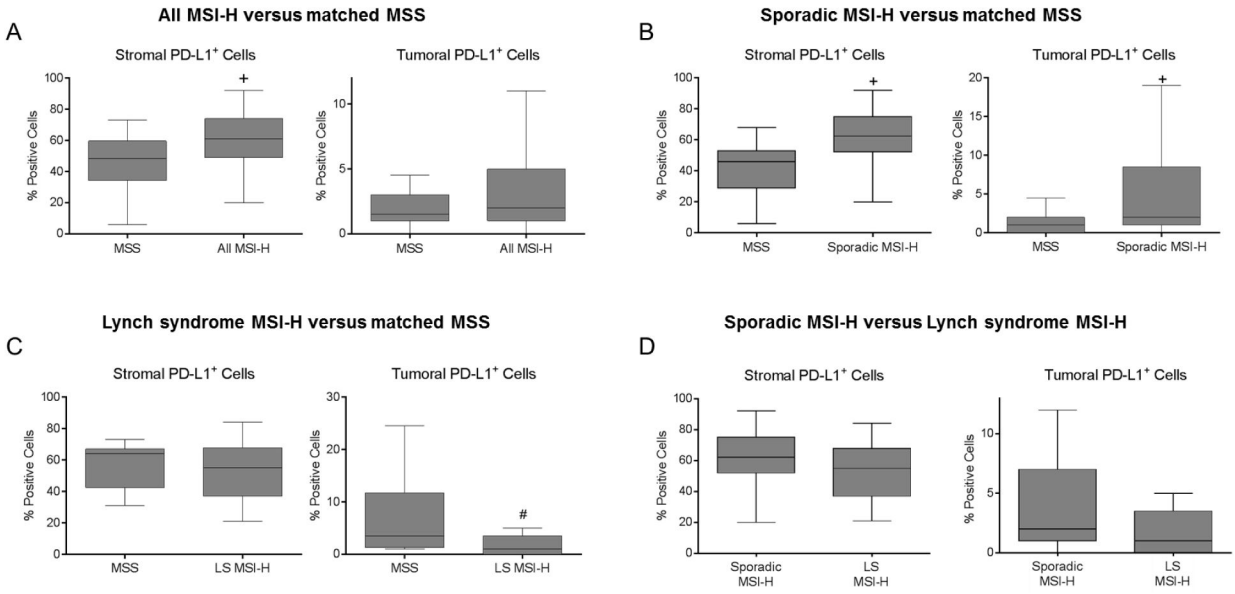

Figure 1. Differences in percentage of PD-L1 expression in MSI-H compared to MSS EC

(A) Comparison of overall MSI-H EC cohort (n=60) versus matched MSS EC (n=96) indicating increased percentage of PD-L1$^+$ cells within the peritumoral stroma, but no significant difference in tumoral PD-L1 staining. **(B)** Sporadic MSI-H EC (n=38) versus matched MSS EC (n=60) also shows increased percentage of PD-L1$^+$ cells within the peritumoral stroma and tumor. **(C)** Comparison of LS MSI-H EC (n=20) versus matched MSS EC (n=25) indicates no difference in percentage of PD-L1$^+$ cells within stroma but a decreased percentage of PD-L1+ cells in the tumor. **(D)** Comparison of sporadic MSI-H (n=38) versus LS MSI-H EC (n=20) indicates no difference in percentage of PD-L1$^+$ cells within the stroma or tumor compartments. The center line of the box plot indicates median. +p<0.01, #p=0.03. Abbreviations: MSI-H, high microsatellite instability; MSS, microsatellite stable; LS, Lynch syndrome.

Table 1

Clinicopathological characteristics by MSI-H and MSS status.

	MSI-H (N=60)	MSS (N=96)	P value
Mean Age (y)	59.7	59.7	0.93
Mean BMI (kg/m^2)	34.2	36.0	0.22
Histology, N (%)			0.33
Endometrioid	56 (93.3)	94 (97.9)	
Undifferentiated	1 (1.7)	1 (1.0)	
Mixed	3 (5.0)	1 (1.0)	
Stage, N (%)			0.76
IA	35 (58.3)	66 (68.8)	
IB	8 (13.3)	15 (15.6)	
II	3 (5.0)	5 (5.2)	
III/IV	9 (15.0)	10 (10.4)	
Unknown	5 (8.3)	--	
Grade, N (%)			0.42
1	6 (10.0)	12 (12.5)	
2	41 (68.3)	73 (76.0)	
3	11 (18.3)	11 (11.5)	
Unknown	2 (3.3)	--	
Depth of Myometrial Invasion, N (%)			0.73
No invasion	8 (13.3)	21 (21.9)	
< 50%	26 (43.3)	49 (51.0)	
≥ 50%	15 (25.0)	26 (27.1)	
Unknown	11 (18.3)	--	
LVSI, N (%)			**0.01***
Present	25 (41.7)	27 (28.1)	
Absent	23 (38.3)	67 (69.8)	
Unknown	12 (20.0)	2 (2.1)	

Abbreviations: BMI, body mass index; kg/m^2, kilograms per meter squared; LVSI, lymphovascular space invasion.

Table 2

Comparison of positive staining cell counts between MSI-H and MSS EC

Marker	All MSI-H EC (N=60) Median # of positive cells/mm^2 (IQR)	MSS EC(N=96) Median # of positive cells/mm^2 (IQR)	P value
Stromal Compartment			
CD8	36.0 (17.3–79.5)	27.2 (7.2–49.6)	0.22
Granzyme B	**74.0 (33.7–166.6)**	**44.2 (18.3–73.8)**	**<0.01** *
CD68	16.9 (3.3–39.4)	18.9 (7.7–36.1)	0.75
PD-L1	**297.9 (238.5–348.7)**	**239.2 (181.9–282.6)**	**<0.01** *
CD3	**87.7 (45.9–119.7)**	**42.5 (42.5–83.3)**	**0.03** *
CD4	**20.2 (11.0–39.0)**	**16.1 (7.8–23.0)**	**0.04** *
CD8$^+$ Granzyme B$^+$	**34.3 (14.2–75.8)**	**21.1 (5.9–37.8)**	**0.01** *
PD-L1$^+$ CD68$^+$	13.8 (2.6–34.6)	9.5 (5.0–21.7)	0.19
CD3$^+$ CD4$^+$	**20.1 (11.0–35.4)**	**16.0 (7.4–22.2)**	**0.04** *
Tumor Epithelial Compartment			
CD8	**5.1 (1.9–10.9)**	**2.8 (0.9–6.9)**	**0.03** *
Granzyme B	**4.9 (2.3–17.9)**	**2.5 (0.9–5.7)**	**0.03** *
CD68	**1.2 (0.2–2.6)**	**1.8 (1.1–3.9)**	**0.02** *
PD-L1	6.8 (2.4–27.6)	7.4 (2.6–14.7)	0.62
CD3	28.1 (12.1–66.0)	27.8 (9.9–44.8)	0.45
CD4	8.4 (3.2–29.1)	10.4 (3.8–18.7)	0.66
CD8$^+$ Granzyme B$^+$	**2.5 (1.0–6.7)**	**1.4 (0.6–3.3)**	**<0.01** *
PD-L1$^+$ CD68$^+$	0.1 (0.0–0.4)	0.1 (0.0–0.3)	0.71
CD3$^+$ CD4$^+$	8.1 (2.9–28.2)	10.3 (3.3–18.5)	0.67

* $p<0.05$.

Abbreviations: MSI-H, high microsatellite instability; MSS, microsatellite stable; EC endometrial cancer; IQR, interquartile range.

Table 3

Comparison of immune cell populations in sporadic MSI-H versus MSS EC.

Marker	Sporadic MSI-H EC(N=38) Median # of positive cells/mm^2 (IQR)	MSS EC (N=60) Median # of positive cells/mm^2 (IQR)	P value
Stromal Compartment			
CD8	35.2 (14.6–54.6)	23.3 (6.8–77.4)	0.85
Granzyme B	**70.8 (41.1–120.7)**	**44.2 (13.4–81.6)**	**0.04** *
CD68	18.6 (8.1–58.8)	17.4 (7.4–30.3)	0.08
PD-L1	**311.1 (260.8–356.1)**	**219.7 (158.6–270.9)**	**<0.01** *
CD3	**87.7 (49.2–121.2)**	**62.5 (37.8–80.8)**	**0.01** *
CD4	**22.1 (13.2–39.1)**	**15.9 (7.9–22.0)**	**0.01** *
CD8$^+$ Granzyme B$^+$	27.3 (13.7–49.5)	22.4 (5.5–44.3)	0.23
PD-L1$^+$ CD68$^+$	**14.8 (4.8–47.9)**	**6.9 (3.9–15.3)**	**<0.01** *
CD3$^+$ CD4$^+$	**22.1 (13.1–36.8)**	**15.8 (7.3–21.7)**	**0.01** *
Tumor Epithelial Compartment			
CD8	4.1 (1.7–10.4)	2.6 (0.8–6.7)	0.37
Granzyme B	5.8 (2.8–19.0)	2.6 (0.7–5.3)	0.05
CD68	1.6 (0.6–3.4)	1.7 (0.9–3.2)	0.31
PD-L1	**10.2 (3.7–38.4)**	**3.9 (1.2–8.9)**	**0.02** *
CD3	32.3 (13.1–68.6)	22.0 (8.7–45.0)	0.17
CD4	9.4 (5.8–30.2)	9.0 (3.5–18.3)	0.23
CD8$^+$ Granzyme B$^+$	2.4 (0.6–5.9)	1.5 (0.6–3.5)	0.06
PD-L1$^+$ CD68$^+$	**0.2 (0.0–0.7)**	**0.1 (0.0–0.2)**	**0.02** *
CD3$^+$ CD4$^+$	9.1 (5.0–29.7)	7.6 (3.1–17.9)	0.23

* $p<0.05$.

Abbreviations: MSI-H, high microsatellite instability; MSS, microsatellite stable; EC, endometrial cancer; IQR, interquartile range.

Table 4

Comparison of immune cell populations in LS MSI-H versus MSS EC.

Marker	LS MSI-H EC (N=20) Median # of positive cells/mm^2 (IQR)	MSS EC (N=25) Median # of positive cells/mm^2 (IQR)	P value
Stromal Compartment			
CD8	**84.9 (21.5–152.5)**	**30.3 (8.6–38.7)**	**0.01** *
Granzyme B	136.0 (30.0–185.4)	48.3 (19.8–75.2)	0.05
CD68	3.5 (0.7–22.0)	34.7 (7.6–47.6)	0.09
PD-L1	267.9 (169.6–328.7)	282.6 (219.3–313.6)	0.83
CD3	84.3 (16.7–136.0)	71.6 (51.3–105.3)	0.92
CD4	16.3 (1.9–33.5)	17.9 (7.6–34.2)	1.0
CD8$^+$ Granzyme B$^+$	**80.7 (13.6–114.1)**	**19.8 (7.4–32.2)**	**0.01** *
PD-L1$^+$ CD68$^+$	2.6 (0.1–20.3)	24.7 (5.9–39.7)	0.21
CD3$^+$ CD4$^+$	16.3 (1.9–33.4)	17.9 (7.4–46.4)	1.0
Tumor Epithelial Compartment			
CD8	**8.1 (3.4–12.8)**	**3.5 (0.9–7.5)**	**0.01** *
Granzyme B	3.9 (2.1–17.3)	2.5 (1.4–6.4)	0.34
CD68	**0.1 (0.0–0.9)**	**2.1 (1.5–4.7)**	**0.01** *
PD-L1	**3.4 (1.0–11.5)**	**15.5 (6.4–41.7)**	**0.02** *
CD3	18.7 (3.8–66.3)	38.8 (23.3–54.0)	0.43
CD4	2.8 (0.3–25.9)	14.2 (9.0–25.8)	0.38
CD8$^+$ Granzyme B$^+$	**3.6 (1.6–7.9)**	**1.4 (0.5–3.5)**	**0.01** *
PD-L1$^+$ CD68$^+$	**0.0 (0.0–0.0)**	**0.3 (0.2–0.5)**	**0.02** *
CD3$^+$ CD4$^+$	2.7 (0.2–25.8)	14.1 (8.7–25.7)	0.37

* $p<0.05$.

Abbreviations: LS MSI-H, Lynch syndrome high microsatellite instability; MSS, microsatellite stable; EC endometrial cancer; IQR, interquartile range.

Table 5

Comparison of positive staining cell counts between sporadic MSI-H and LS MSI-H EC

Marker	Sporadic MSI-H EC (N=38) Median # of positive cells/mm^2 (IQR)	LS MSI-H EC(N=20) Median # of positive cells/mm^2 (IQR)	P value
Stromal Compartment			
CD8	**34.2 (13.9–52.2)**	**82.8 (22.1–151.3)**	**<0.01** *
Granzyme B	67.5 (36.5–113.6)	138.8 (31.4–206.6)	0.29
CD68	**18.6 (9.2–48.1)**	**3.6 (0.8–27.9)**	**0.04** *
PD-L1	297.9 (264.1–352.3)	289.3 (200.0–338.7)	0.34
CD3	84.6 (52.3–114.1)	84.3 (16.7–136.0)	0.82
CD4	22.1 (13.1–39.0)	16.3 (1.9–33.5)	0.30
CD8$^+$ Granzyme B$^+$	**27.5 (13.7–46.7)**	**79.1 (14.5–103.9)**	**0.01** *
PD-L1$^+$ CD68$^+$	**14.8 (6.0–41.4)**	**2.7 (0.2–25.8)**	**0.04** *
CD3$^+$ CD4$^+$	22.1 (13.1–35.4)	16.3 (1.9–33.4)	0.31
Tumor Epithelial Compartment			
CD8	4.2 (1.9–9.9)	8.2 (3.7–17.5)	0.08
Granzyme B	4.9 (2.8–17.9)	6.4 (2.2–34.1)	0.99
CD68	**1.4 (0.4–3.1)**	**0.1 (0.0–1.0)**	**<0.001** *
PD-L1	8.2 (3.6–35.7)	4.8 (1.3–17.0)	0.18
CD3	30.0 (12.6–66.0)	18.7 (3.0–66.3)	0.23
CD4	8.6 (5.5–29.1)	2.8 (0.3–25.9)	0.06
CD8$^+$ Granzyme B$^+$	2.6 (0.8–6.2)	3.7 (1.6–10.7)	0.23
PD-L1$^+$ CD68$^+$	**0.1 (0.0–0.6)**	**0.0 (0.0–0.1)**	**<0.01** *
CD3$^+$ CD4$^+$	8.3 (4.7–28.2)	2.7 (0.2–25.8)	0.07

* $p<0.05$.

Abbreviations: MSI-H, high microsatellite instability; LS, Lynch syndrome; EC endometrial cancer; IQR, interquartile range.